Nigerian Research Journal of Chemical Sciences **(ISSN: 2682-6054)**
Volume 10, Issue 2, 2022

Binding of Ag(I) ions to DNA nucleobases: A mechanistic study

Hector Henry Oyem

Department of Chemical Sciences, University of Delta, Agbor, Delta state, Nigeria

Email: hector.oyem@unidel.edu.ng; hectoroyem@yahoo.co.uk

ABSTRACT

A mechanistic approach to the reaction between Ag(1) ions and DNA nucleobases was proposed in this study with ^{1}H, and ^{31}P NMR analytical tools to back up the mechanisms. The proposed reaction mechanisms is based on the stability of the resulting products and the lowering of the free energy occasioned by the delocalization of electrons and the extent and spread of charge(s) on the nucleobases upon Ag(1) addition. Solutions of DNA nucleobases were treated with silver nitrate solution in a ratio of 1:2 in aqueous medium and reduced by equivalent portions of sodium borohydride. Similarly, for the NMR analyses, the same protocol was repeated using deuterium oxide solution as the reaction medium. Spectra obtained were used to support the proposed reaction mechanisms for the binding characteristics of Ag(1) ions on DNA bases. Results support the assumption that Ag(1) ions bonded to DNA bases at the **A**N3 **A**N7, **C**N3, **G**N7 positions with the electrophilic attack centred on the lone pair electrons on these nitrogen atoms. Consequently, the resulting electron delocalization and spread of charge(s) caused significant deshielding of the **A**H8, **C**H6, **G**H8 and the **C**H1' (ribose sugar) protons. The carbonyl oxygen atom was not the favoured binding site of Ag(1) ions as was illustrated with thymine molecule; as ^{1}H NMR spectra did not support this assumption. Similarly, ^{31}P NMR spectra showed that Ag(1) ions did not bind with the nucleobases at the phosphate oxygen atoms. Whereas, prominent emission bands were observed after reduction of the Ag^{+}-DNA nucleobases with $NaBH_4$, weak emission band was recorded after the reduction of Ag(I)-thymine complex. It was concluded that Ag(I) ions bonded with thymine, *albeit* weakly, because the **T**N3 is saturated. In all, delocalization of electrons and spread of charges led to a more profound deshielding effect on cytosine.

Keywords: DNA nucleobases, Ag(1) ions, ^{1}H NMR, delocalization, charge spreading.

INTRODUCTION

Nanoparticles are materials whose dimensions are in the 1 to 100nm range [1–4]. Metal nanoparticles are usually prepared from the metal salt precursors often in aqueous solutions and reducing them with an appropriate reducing agent. Once formed, nanoparticles grow rapidly into larger particles because of their large surface energy [3–5]. For this reason,

stabilizers are required in the form of ligands to stem the growth and aggregation of the nanoscale particles.

Nanoparticles are different from nanoclusters, with the latter being smaller than the former in having much fewer number of atoms usually less than 2 nm [6,7]. This low density of state exhibited by nanoclusters make them have their characteristic bandgaps and thus display interesting opto-physical properties including fluorescence [8]. The uniqueness of these clusters is their dramatic change in physical properties upon the addition of one single atom. This phenomenon is what is now known as the magic number effect.

Nanoclusters similarly need stabilizing ligands to control their spontaneous growth and aggregation. Capping ligands of many kinds have been associated with nanoparticles, typical among them is deoxyribonucleic acid (DNA). DNA is the genetic material which is present in the chromatin of eukaryotic cells. Its array of nucleobases with numerous functional sites strung along the backbone of ribose sugar and phosphate groups [9–12] make it the ideal templating material for stabilizing nanoparticles against growth, thereby preserving their desired optical properties.

Single-stranded DNAs also known as oligomers are the most widely employed in this respect [13]. The nitrogen-containing nucleobases are the sites of metallic bonding on DNA molecules [14,15]. The lone pair of electrons on these nitrogen atoms are the centre of electrophilic attack by metallic electrophiles. These binding sites are present on the four DNA bases of adenine, cytosine, guanine, and thymine [10,16]. Cytosine and thymine both possess pyrimidine rings whereas, adenine and guanine contain the purine rings.

Although, researchers have come to identify the biding sites of metal ions on DNA molecules by using several analytical techniques, however, there is hardly any account in the literature where the mechanism of this binding processes were actually explained. In this present study, attempt is made to fill in this gap by demonstrating through mechanistic pathways the nanoclusters-DNA capping ligand formation. Taking into cognizance the extent of delocalization of electrons by the in-coming substituent metal ion (electrophile), and the ability of the electrophile to spread the charge in the resulting specie so as to lower the free energy. While using ^{1}H and ^{31}P nuclear magnetic resonance (NMR) as well as fluorescence spectroscopy techniques to buttress the proposed theory/argument.

MATERIALS AND METHOD

Materials

Silver metal is often the choice in many instances because of its relative photostability and interesting optical properties. Silver nitrate salt ($AgNO_3$, 99 %) (D1685-100G) was bought from Sigma-Aldrich, USA. Sodium borohydride ($NaBH_4$, 99 %) (213462-25G) also from Sigma-Aldrich, USA. Adenosine 5'-monophosphate disodium salt (≥ 99%), guanosine 5'-monophosphate disodium salt hydrate (≥ 99%), cytidine 5'-monophosphate disodium salt (≥ 99%), thymidine 5'-monophosphate disodium salt hydrate (≥ 99%); nucleotides all products of Sigma-Aldrich. Deuterium oxide (D_2O 99.96 %), Sigma-Aldrich, a product of USA. All chemicals were used as purchased without further treatment. Nanopure water obtained from, Millipore Diamond Barnstead series 1370, model D11931, operated at 100-240V, with a resistivity of 18.2 MΩ-cm. 500 µL Hellma micro-quartz cuvette with all four clear sides (path length - 10 mm).[2] All reagent were used as purchased without any further treatment.

Instrumentations

Ultraviolet-Visible Spectrophotometer (UV-Vis spectrophotometer)

UV-Vis absorption spectra of the AgNCs were obtained using Varian Cary 100 Bio spectrophotometer with a tungsten halogen visible source, and a deuterium arc ultraviolet lamp. The detector was an R928 (PMT) photomultiplier detector, the maximum scan range was 190 – 900 nm, using a 500 µL quartz microcuvette (Hellma UK Ltd).

Fluorescence Spectrophotometer

Fluorescence emission and excitation spectra were recorded with a SPEX FluoroMax ™ spectrofluorimeter instrument, New Jersey, USA. The excitation source was an ozone-free xenon lamp with a photomultiplier and photodiode as the emission and reference detectors respectively. The emission/excitation scan range of 200-950 nm in the ultraviolet and visible regions.

Nuclear magnetic resonance (NMR)

The spectrometers used were a Bruker 500 and 700 MHz Avance III HD with 11.7 Tesla spectrometer for the 500 MHz, an auto-sampler, with 5 and 10 mm probes range for virtually all active NMR nuclei. Chemical shifts are reported in ppm referenced to TMS (trimethylsilane) and run with suppression of the H_2O frequency at 4.7 ppm. While the ^{31}P spectra were obtained from the 500 MHz instrument operating at 202.46 MHz with an external reference of 85% phosphoric acid (H_3PO_4).

Methods

Syntheses of silver nanoclusters (Ag NCs) on adenosine, cytidine, guanosine, and thymidine 5'-monophosphate template in aqueous solution

Exactly 1 mg (0.0010 g) each the nucleotide salts was dissolved in 1 mL deionised water to form stock solutions of 2.56, 2.72, 2.46, 2.73 mM of adenosine, cytidine, guanosine, and thymidine 5'-monophosphate stock solutions respectively. From each of these 1 mL stock solutions, 0.5 mL solutions each of 0.256, 0.272, 0.246, and 0.273 mM accordingly of these nucleobases were reacted with 0.5 mL portions of 0.128, 0.136, 0.123, & 0.683 mM Ag(I) concentrations respectively in a 1:2 Ag:base ratio; shaken for 2 minutes and then allowed to stand wrapped in aluminium foil in a dark cupboard for 30 minutes. Afterwards, they were subsequently reduced with equivalent portions (0.5 mL) of aqueous $NaBH_4$ solution in a 1:1 Ag^+: BH_4^- stoichiometric ratio. In all, the total reaction volume was 1.5 mL for each nucleotide.

Syntheses of Ag NCs on adenosine, cytidine, guanosine, and thymidine 5'-monophosphate disodium salts in D2O for NMR analyses

From each of the salts of these nucleoside, 1mg (0.0010 g) was dissolved in 1 mL D_2O to form stock solutions of 2.56, 2.72, 2.46, 2.73 mM of adenosine, cytidine, guanosine, and thymidine respectively. From each of these, 0.4 mL were put in NMR tubes and taken for ^1H, and ^{31}P NMR analyses. After which they were then reacted with 100 µL D_2O portions of 0.128, 0.136, 0.123, & 0.683 mM Ag(I) concentration in a 1:2 Ag:base ratio. These were shaken for 2 minutes and then allowed to stand wrapped in aluminium foil-paper in a dark cupboard for 30 minutes before being studied by ^1H, and ^{31}P NMR analyses. They were subsequently reduced with equivalent 100 µL portions of $NaBH_4$ in D_2O solution in a 1:1 Ag^+: BH_4^- ratio to form DNA-bound AgNCs before repeating the ^1H, and ^{31}P NMR analyses. All reactions took place under the constant atmosphere of argon gas.

Furthermore, 40 µL of the samples were pipetted into a 500 µL micro-quartz cuvette and made up with nanopure water for optical measurements.

RESULTS AND DISCUSSION

Mechanisms of electrophilic reaction between Ag(I) ions and DNA nucleobases

Binding of Ag(I) ions with adenine

Adenine is one of two DNA nucleobases with the purine ring. The purine ring comprises the pyrimidine and imidazole rings fused together. It has four nitrogen atoms on the molecule in 1, 3, 5, and 7 with an amine ($-NH_2$) group attached as a substituent group on the carbon atom

in the number 6 position of the pyrimidine component of the purine ring. Usually the nitrogen atom carries a pair of lone pair of electrons which are not involved in bonding. These often are the sites for electrophilic reagents like Ag(I) ions in this case [14,17,18]. On the adenine molecule, the nitrogen atoms in positions 1 and 7 are the preferred sites for electrophilic attacks with Ag(I) ions.

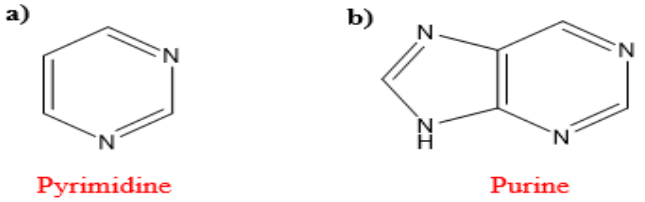

Figure 1: Structure of pyrimidine and purine rings of DNA nucleobases

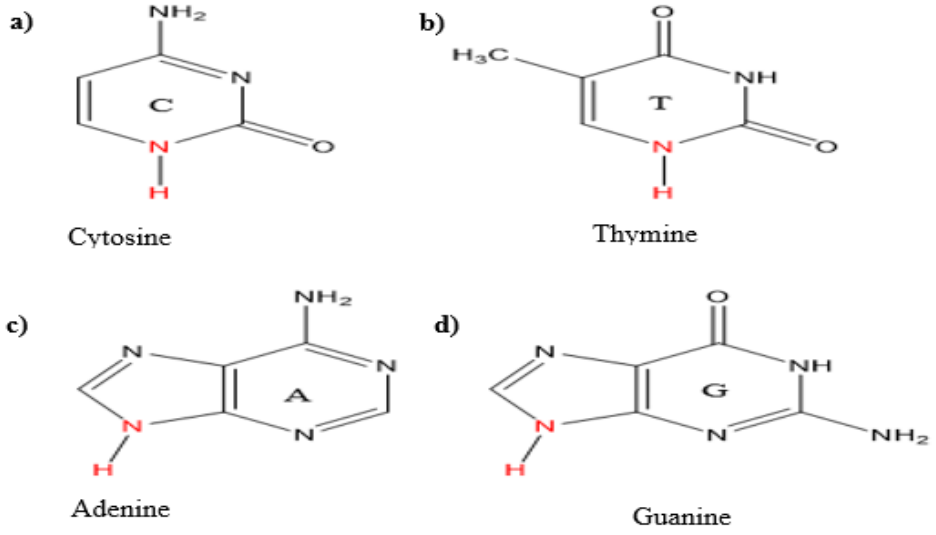

Figure 2: The structural formula of the four DNA nucleobases

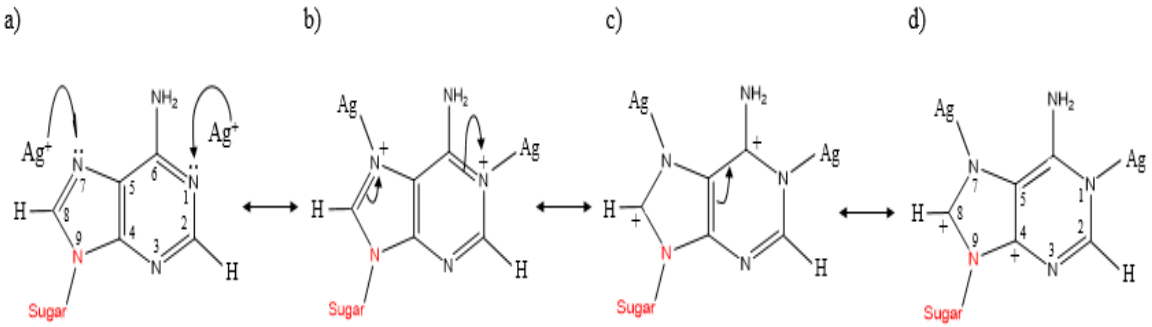

Figure 3: Mechanism of electrophilic attack by Ag^{+} ion on adenine nucleobase

There are four nitrogen atoms on the purine ring in adenine nucleobase at position 1, 3, 7, and 9, two of these, **A**N1 and **A**N7 are favourable sites for binding with Ag(I) ions. The lone pair of electrons on nitrogen atoms are the electron-rich centres and sites of attractions for electrophilic reagents.

Ag(I) ions attack adenine at the **A**N1 and **A**N7 positions and so forms a new bond with these nitrogen atoms via the lone pair electrons. These nitrogen atoms then carry a resultant positive charge, thereby, leading to the delocalization of the pi-electrons between carbon and nitrogen (C6 and N1) to neutralise the positive charge on N1 created from the bonding of Ag and **A**N1. A carbonium ion is formed as the positive charge spreads from N1 to C6 on the adenine purine ring. Delocalization of the second pi-electrons between C4 and C5 occurs as the positive charge spreads further from C6 to C4 of the pyrimidine ring in adenine with the pi-electron being delocalized to between C5 to C6. We could expect delocalization to continue onto the **A**N3 atom and then to **A**C2 which should cause a deshielding of the **A**H2 proton. That would result in a downshift (higher frequency) of the **A**H2 signal from its initial chemical shift position before the reaction with Ag(I) ions. However, evidences in the ^{1}H NMR data reported in fig. 12 did not supported this argument. There was no chemical shift in the position of the **A**H2 protons after reacting with Ag(I) ions or even after reduction. In other words, the **A**H2 signal was neither displaced up- or downfield of the reference standard, trimethylsilane (TMS) irrespective of the reaction with Ag(I) ions. Meanwhile, observations of the **A**H8 signals show clearly the obvious displacement of the **A**H8 signal further downfield of TMS after treating with Ag(I) ions. This is evident in the ^{1}H NMR spectra of adenosine 5' mononucleotide presented in fig. 12b, thus confirming that delocalization and spreading of the positive charge stopped at the **A**C4 atom in the pyrimidine ring.

In the case of the **A**H8 signal, it is obvious that the binding of Ag(1)ion to the **A**N7 again results in the formation of a new bond between Ag and N7 and the consequent formation of a positive charge formed on the N7 atom on the imidazole component of the purine ring in adenine nucleobase. The presence of this positive charge caused a delocalization of the pi-electrons between **A**N7 and **A**C8 to the positively charged **A**N7 atom resulting in the formation of a carbonium ion on the **A**C8 atom. This is believed to have caused the notable chemical shift in the **A**H8 signal in the ^{1}H NMR spectra upon the addition of Ag(I) ions to adenine nucleobase. The subsequent reduction of the Ag(I)-adenine co-ordination complex restored the electron cloud around the **A**C8 and the **A**H8 thereby leaving the **A**H8 proton shielded. The consequence of which is the return of the **A**H8 signal back to its original chemical shift position.

Binding of Ag(I) ions to cytosine

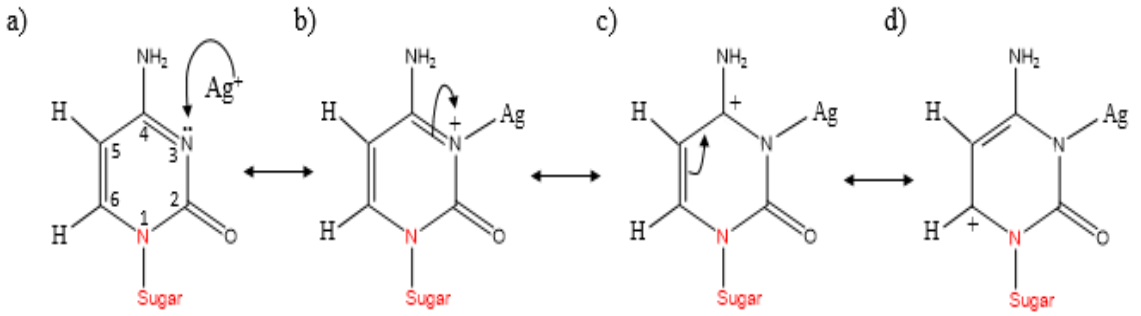

Figure 4: Mechanism of electrophilic attack by Ag^+ ion on cytosine nucleobase

Cytosine is a nucleobase having the pyrimidine ring. It possess two nitrogen atoms at **C**N1 and **C**N3, the latter being the more likely site for bonding with Ag(1)ion. Silver binds by co-ordinate bonding with the nitrogen atom (**C**N3) curtesy of the lone pair electron in an electrophilic reaction. Again, a positive charge is similarly formed on the CN3 atom causing the delocalization of pi-electrons on **C**N3 and **C**H4, thereby creating a carbonium ion at **C**C4. Further delocalization of the second pi-electrons between **C**H5 and **C**H6, and spreading of the positive charge occurred in the bid to lowering the energy of the molecule. Eventually, the positive charge is spread onto the **C**C6 (carbonium ion) making the **C**H6 deshielded and exposed to the effects of the strong magnetic field.

In spite of the extent of electron delocalization in cytosine, the **C**H5 remained shielded by the pi-electron cloud between **C**C4 and **C**C5. Conversely, the **C**H6 is rather deshielded and a higher chemical shift position of its signal is observed. This is contrary to the **C**H5 which is neither displaced up- nor downfield of TMS (fig. 13b) after the reaction with Ag(1) ions. Reduction of Ag (I)-cytosine co-ordination complex restored the electron cloud at the **C**C6 (carbonium ion) and the **C**H6 proton became shielded as demonstrated by the return of the signal to its initial chemical shift position. Meanwhile, the H1' signal was also slightly shifted downfield of TMS following the addition of Ag(1) ions to cytosine. This was the only case of such shift in the H1' signal of the ribose sugar component of DNA of all the nucleobases studied.

Considering that cytosine and thymine are both pyrimidine analogues of DNA nucleobases, a comparative analysis of the ^{1}H NMR of these nucleobases revealed that the binding of Ag (1) ions to **C**N3 caused electron delocalization and the spreading of the resulting positive charge. It is believed that the delocalization of the positive charge stopped at the **C**C6

carbonium cation on to which the **C**H6 is attached, otherwise the slight displacement of the initial **C**H6 signal in the ^{1}H NMR spectrum would have been absent if the charge had spread further to the **C**N1 position. The spreading of the positive charge started at the **C**N3 position and ended at the **C**C6 position, hence the ^{1}H NMR signal for **C**H6 occurred at a higher chemical shift position from its initial position prior to the reaction with Ag(1)ion. Consequently, the displacement of the H1' signal is thought to have been effected by a similar deshielding of the H1' of the ribose sugar, a situation not observed in the spectra of the other three nucleobases.

This shifting of the H1' signal was therefore attributed to the mesomeric effect of the nearby carbonyl oxygen atom (**C**C2) which accounts for the electron-withdrawing inductive effect that extended through the **C**N1 down to the H1' of the ribose sugar. This phenomenon was not reported with thymine in the NMR range studied.

However, it is not certain at this point if the mesomeric effect of the carbonyl oxygen resulted in bonding between cytosine and Ag(1)ion, and if the resulting Ag-O bond (if formed) was stable even after reduction. This would require confirmation by comparing infra-red spectra of cytosine before and after reacting with Ag(1) ions, and also post-reduction to see if the carbonyl functional group between 1650 – 1800 cm^{-1} subsists or not.

Binding Ag(I) ions with guanine

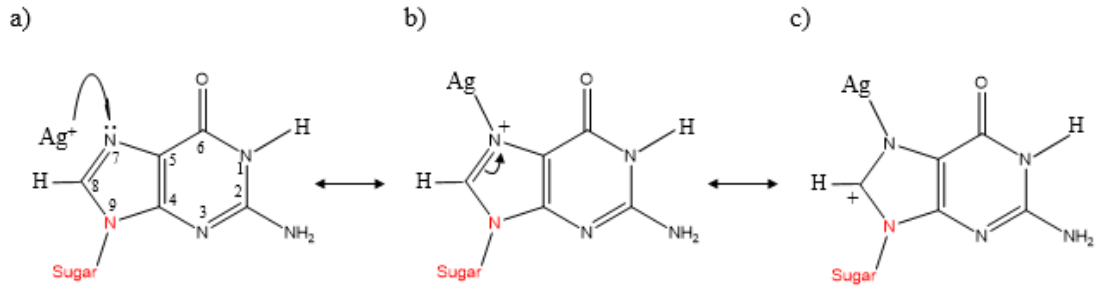

Figure 5: Mechanism of electrophilic attack by Ag^{+} ion on guanine nucleobase

Guanine nucleobase is the second member of the purine ring nucleobases after adenine but unlike the former, guanine has one (**G**N7) site for possible electrophilic attack by Ag(1)ion. Electron delocalization and charge transfer in the guanine molecule appears restricted sort of, to the imidazole (purine) ring and does not involve the pyrimidine ring like was the case with adenine.

Electrophilic attack by Ag(1)ion took place on the **G**N7 position of the molecule with a corresponding positive charge on the same **G**N7 position as Ag (I)-guanine co-ordinate complex was formed. In order to reduce the energy of the resultant molecule, pi-electrons between **G**N7 and **G**H8 are delocalized to the positively charge N7 atom. This similarly creates a carbonium ion on **G**C8 which results in the displacement of the electron cloud in this region, creating a deshielding effect on the **G**H8 proton. Expectedly, the reaction ^{1}H NMR spectra of the Ag (I)-guanine complex would show a chemical shift of the **G**H8 proton further downfield of TMS. This is exactly the results obtained in the spectra displayed in figure 14b after reacting Ag(1) ions with guanine 5' mononucleotide. Besides this **G**H8 proton, there are no other methylenic (-CH_2) protons in the molecule unlike the case of **A**H2 in adenine.

The other protons on the guanine molecule belong to the amine (imino) group which have chemical shift positions far in the region of 11. 0 to 15.0 downfield of TMS. Researchers believe that these (amine) nitrogens are not the preferred sites of electrophilic attacks [19–21] by Ag(1) ions, hence, focus is placed on the nitrogen 1 and 3, of the pyrimidine nucleobases, and the nitrogen 1, 3, 7, and 9 of the purine nucleobases [20–22]. Yet again, evidence from the NMR spectra in this study point at Ag(1) ions binding preferably with the DNA nucleobases at the **A**N1, **C**N3, **A**N7, and **G**N7 positions which are associated with some degree of unsaturation, but not for thymine.

Binding of Ag(I) ions with thymine

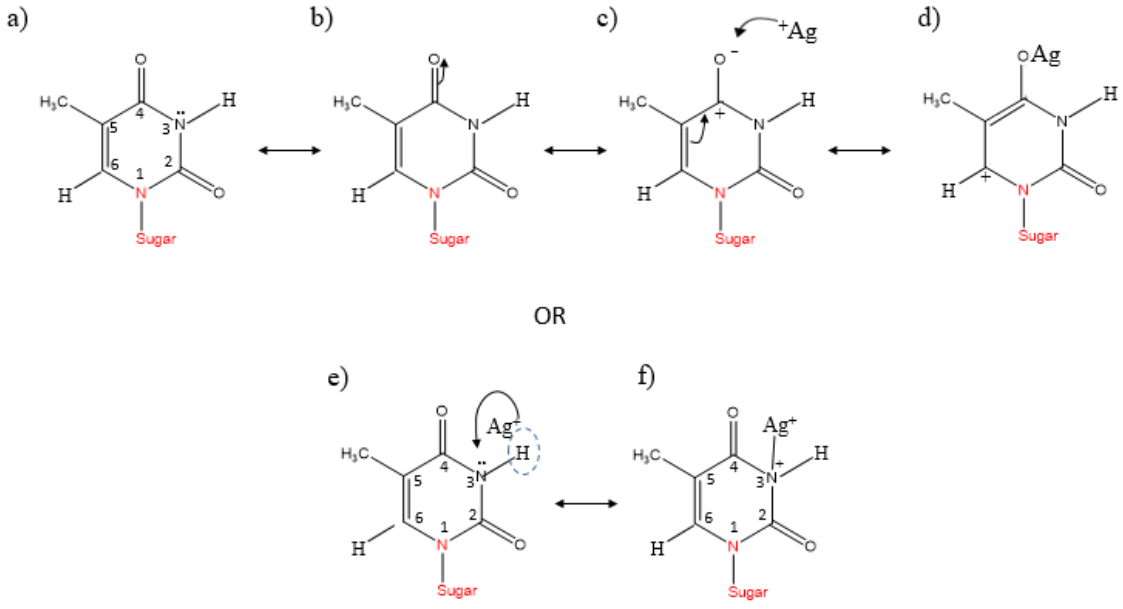

Figure 6: Mechanism of electrophilic attack by Ag^{+} ion on **T**N3 position of thymine nucleobase

From a structural perspective, the reaction of Ag(I) ions with thymine nucleobase would be anticipated to be a difficult one, this is because the **T**N3 nitrogen atom is already saturated. Here, the N3 position unlike in the case of cytosine is bonded to an H-atom in the form of an amine (2^o amine). Even with the presence of the lone pair electron on the N3 of thymine (**T**N3), an electrophilic attack by Ag(I) ion on this site was not considered feasible because of this saturation. However, the result of the fluorescent spectrum demonstrated that Ag(I) ions bonded with thymine. A co-ordination complex may have therefore resulted from this reaction without the displacement of the **T**N3 (imino) hydrogen atom by Ag(I) ion. This is believed to explain the diminishing of the proton signals which would be observed in the ^{1}H NMR spectrum in figure 13b following the addition of Ag(I) ions to thymine in the subsequent section.

Considering an attack on the carbonyl oxygen at position **T**C4 arising from the delocalization of the pi-electron of the carbonyl group to the carbonyl oxygen (fig. 6b), this could lead to the electrophilic attack by Ag(I) ion on the carbonyl oxygen atom (fig. 6c) and the subsequent formation of a carbonium ion on **T**C4. The delocalization of the pi-electron between **T**C5 and **T**C6 to **T**C4 and **T**C5 could occur thereby spreading the positive charge further to **T**C6. Consequently, as the electron cloud is shifted away from this **T**C6 position, the **T**H6 proton would be left even more deshielded. Ordinarily, this should cause the **T**H6 signal to shift to higher chemical shift position as the outcome of the addition of Ag(I) ion to thymine molecule (fig. 6d), as was reported with cytosine. But this was not supported by the ^{1}H NMR data as would be seen in Figure 13 below.

Similarly, the situation which was observed with cytosine resulting in the displacement of the H1' signal downfield should have also been observed with thymine since there is a similar presence of electron-withdrawing mesomeric carbonyl oxygen at the **T**C2 position. Thus, creating an inductive effect whose influence should be transmitted all through the **T**N1 to the H1' proton. As interesting as this mechanism may seem, this did not happen with thymine! This hypothesis was clearly not supported by the ^{1}H NMR data obtained for thymine in this study, ostensibly contrasting with that of its cytosine (pyrimidine) analogue above.

Analytical tools in support of these reaction mechanisms

The following analytical tools were used to confirm the mechanisms of the reaction of Ag(I) and DNA nucleobases. These among other analytical tools are able to provide credible evidence in support of bond formation through the appearance or disappearance of certain

characteristic signals at exact positions or away from such hitherto known positions due to the attachment of substituent groups to the original molecule.

Nuclear magnetic resonance spectroscopy

Nuclear magnetic resonance (NMR) is an important tool in the study of the signals of certain nuclei in the presence of strong magnetic fields. The signals of these nuclei are measured against those of a particular reference standard according to the NMR type, and their chemical shift positions as well as the broadening or flattening out of peak intensities determined.

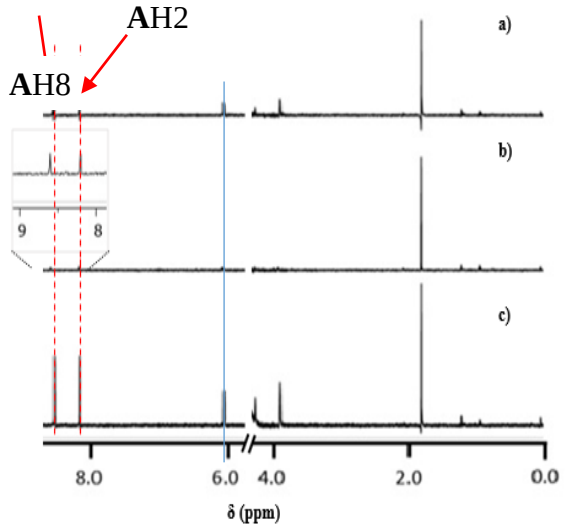

Figure 7: ^{1}H NMR spectra of a) adenosine b) adenosine_Ag^{+} complex and c) adenosine_Ag^{0}. All spectra acquired at 298 K in D_2O with tetramethylsilane (TMS) as a reference (Source: Oyem, [23])

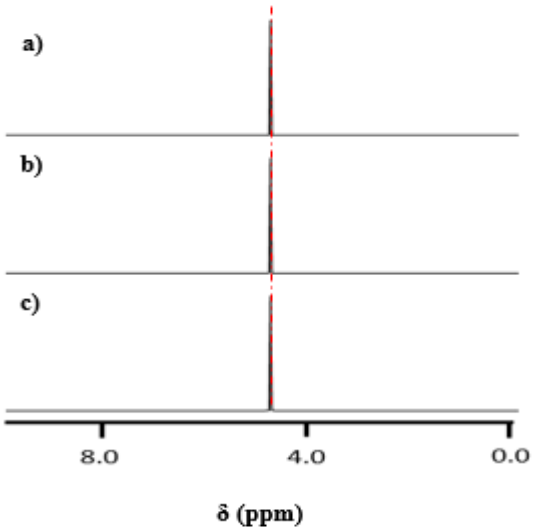

Figure 8: ^{31}P NMR spectra of a) adenosine b) adenosine_Ag^{+} complex and c) adenosine_Ag^{0} in D_2O at 298 K with 85 % phosphoric acid as a reference (Source: Oyem, [23])

In this study, ^{1}H and ^{31}P NMR spectra of DNA nucleobases before, after reacting with Ag(I) ions, and then reducing the DNA – Ag(I) complexes with equivalent portions of sodium borohydride ($NaBH_4$) in deuterium oxide solution are examined. The three spectra obtained for each of the DNA nucleobases, the Ag(I) – DNA nucleobases co-ordination complexes, as well as their reduction spectra were stacked together and compared for analytical purposes. Thus, chemical shift (signal) displacement up- or downshift from the reference were clearly observed. Apart from these, the broadening and in some cases outright flattening out of NMR signals were similarly noticed. These put together aided the elucidation and comprehension of the mechanistic steps of the reaction, its feasibility, and in effect, the inevitability of the reaction products.

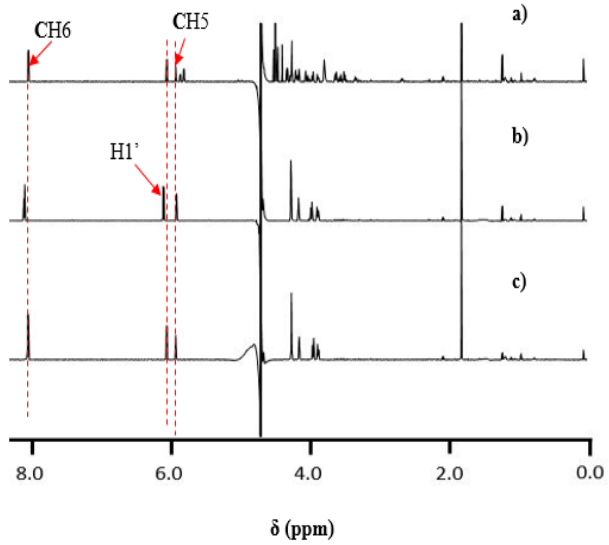

Figure 9: ^{1}H NMR spectra of a) cytidine b) cytidine_Ag^{+} complex and, c) cytidine_ Ag^{0}. All spectra acquired at 298 K in D_2O with tetramethylsilane (TMS) as a reference. (Source: Oyem, [23])

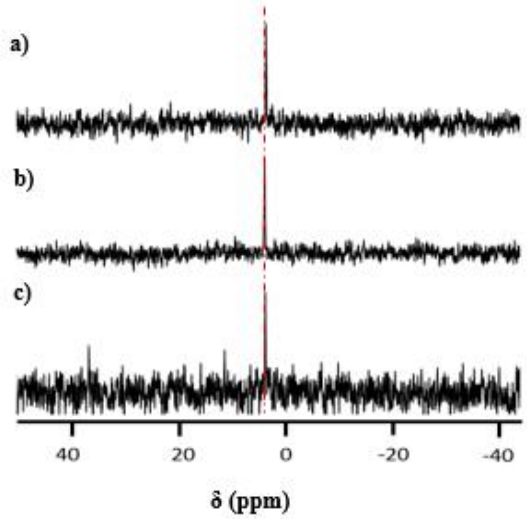

Figure 10: ^{31}P NMR spectra of a) cytidine b) cytidine_Ag^{+} complex and c) cytidine_ Ag^{0} in D_2O at 298 K with 85 % phosphoric acid as a reference. (Source: Oyem, [23])

Note that for the reactions to proceed and a stable product formed (silver-bound DNA nanoclusters), there must be a lowering of the Gibb's free energy [24]. This thermodynamic condition has to be satisfied otherwise, the reaction would not proceed, and no new (whether AgNCs or AgNPs) would be formed.

In figures 7, 9, 11, and 13, figures 7a, 9a, 11a and 13a are the spectra of four DNA nucleobases prior to the reaction with Ag(I) ions. These together show signals of the various protons in the molecules of these DNA mononucleotides at different chemical shift positions relative to TMS. While figures 7b, 9b, 11b, and 13b are ^{1}H NMR spectra of each of these DNA mononucleotides with solutions of Ag(I) ions in a 1:2 molar proportion at room temperature. From these figures, we see slight shifts of about 0.2 ppm in the aromatic proton signals of these DNA types after treating with Ag(I) ions. These shifts of the proton signal positions were considered as evidence of the successful bonding of Ag(I) ion to the nucleobases. Such shifts in proton signals have already been reported by several scholars [19,21]. Meanwhile, in the case of adenosine and guanosine, these signals almost flattened out completely when Ag(I) ion was added to the individual DNA solutions. Note, that the flattening out of ^{1}H NMR signals are veritable signs of spin-spin relaxation and exchange interaction between pairs of magnetic nuclei [25,26] or conformational changes [27].

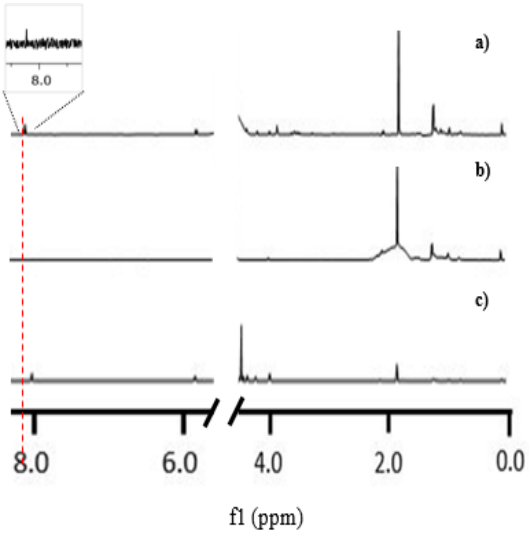

Figure 11: ^{1}H NMR spectra of **a)** guanosine **b** guanosine _Ag^{+} complex and **c)** guanosine _ Ag^{0}. All spectra acquired at 298 K in D_2O with tetramethylsilane (TMS) as a reference (Source: Oyem, [23])

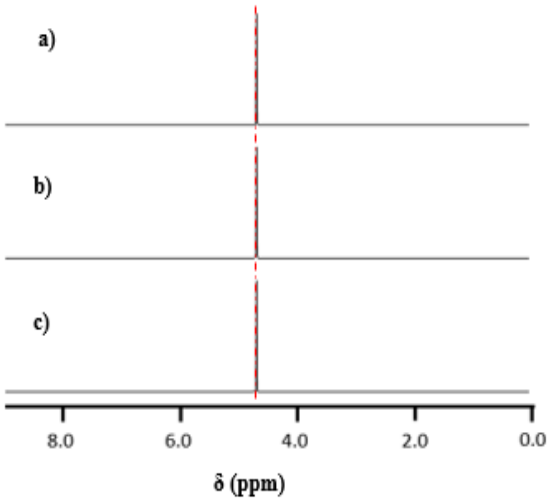

Figure 12: ^{31}P NMR spectra of a) guanosine b) guanosine _Ag^{+} complex and c) guanosine _ Ag^{0} in D_2O at 298 K with 85 % phosphoric acid as a reference (Source: Oyem, [23])

In figures 7c, 9c, 11c and 13c, spectra of Ag-bound DNA nucleobases formed after the reduction of Ag(I)-DNA complexes. After the reduction of these Ag-DNA conjugates, the signals of adenosine and cytidine generally returned to their initial positions. But in guanosine, these signals were shifted a little further upfield (lower frequency) of TMS, an observation which translates to further shielding of the aromatic protons. Whereas, the signals of thymidine protons diminished upon reacting with Ag(I) ions in figure 13b, no change in chemical shift positions were observed. Such occurrences again, are associated with exchange interactions between magnetic nuclei. However, after reduction of the Ag(I)-thymidine complex, these signal intensities were restored.

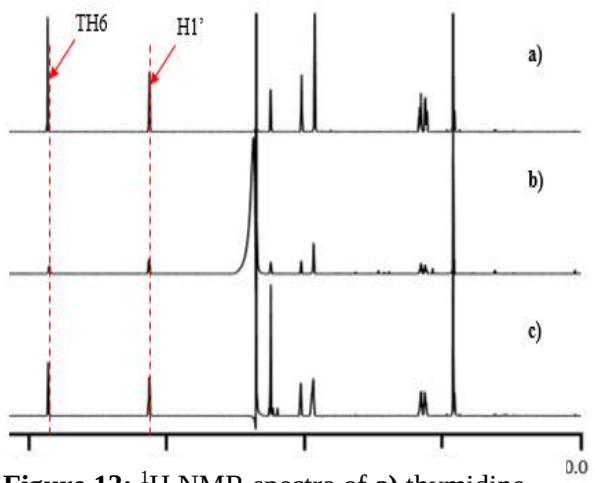

Figure 13: ^{1}H NMR spectra of **a)** thymidine **b** thymidine _Ag^{+} complex and **c)** thymidine _ Ag^{0}. All spectra acquired at 298 K in D_2O with tetramethylsilane (TMS) as a reference (Source: Oyem, [23])

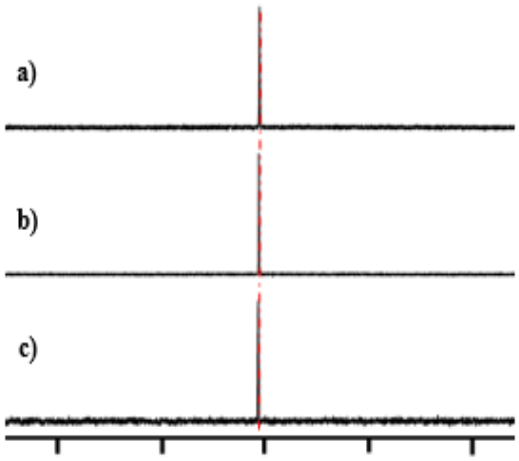

Figure 14: ^{31}P NMR spectra of a) thymidine b) thymidine _Ag^{+} complex and c) thymidine _ Ag^{0} in D_2O at 298 K with 85 % phosphoric acid as a reference (Source: Oyem, [23])

markers of a successful bonding between Ag(I) ions and DNA nucleobases but only as evidences of proton exchange interactions of chemically equivalent nuclei. But more significantly, the shifting of the proton signals downfield of TMS after the reaction of Ag(I) ions with the DNA bases is more decisive in diagnosing that strong bonding has indeed taken place between Ag(I) ions, adenosine, cytidine, and guanosine.

In all of the reactions of Ag(I) ions and DNA nucleobases, only the reaction with thymine did not show any shift in the positions of the aromatic protons in the chemical shift range observed as can be seen on the ^{1}H NMR spectra. All three others show a change in chemical shift positions upon reacting with Ag(I) ions or after reduction. This gives credence to the mechanism proposed in figure 6e and 6f above rather than those of figures 6a to 6d to explain the observations in the reaction between Ag(I) ions and thymidine. It appears that Ag(I) ions may have bonded on to thymine through the TN3 (nitrogen) lone pair electrons in the form of a weak coordinate bonding.

In all the ^{31}P NMR spectra obtained in this study (figures 8, 10, 12, and 14) none of them showed the slightest shift ^{31}P NMR signal position after the reaction with Ag(I) ions and even after reduction. Neither was there any broadening of these ^{31}P NMR signals in all the samples analysed in this study. Peak broadening are a result of conformational changes in the structure of a DNA molecule. And in DNA – metal ions interactions, such conformational changes are often associated with the attachment of metal ions to DNA backbone [12,28]. The interpretation

from these findings typically suggest that Ag(I) ions did not bind with either the carbonyl or any of the phosphate oxygen atoms of the DNA nucleobases.

Uv-vis and Fluorescence Studies

Ultra-violet and visible spectroscopy results of the Ag0 – DNA nucleobases were studied and results presented below. Uv-vis spectra for adenosine and thymine (figures 16 and 17) only show the characteristic DNA peaks at 260 nm wavelength. The absence of any other peak on the Uv-vis spectra is an indication of the absence of large silver nanoparticles (AgNPs). Their presence would have been indicated by the appearance of a plasmon peak around 420 nm. This confirms that AgNPs were not produced with these nucleobases.

The fluorescence spectra of the Ag – DNA nucleobases showed fluorescence peaks between 425 – 435 nm. The appearance of these fluorescent bands is a demonstration of the fact that small AgNPs – precisely, AgNCs have been formed[29]. This is justified by the absence of plasmon bands in the uv-vis spectra of the samples in figures 16 (a) & (b). The wavelength position of these fluorescent bands illustrates that small clusters of Ag are present going by the amount of energy (270 eV) involved at this emission wavelength (430 nm).

Since the uv-vis and emission data for cytosine and guanosine were lost, nonetheless, results of similar study at the same metal-to-DNA base ratio by Ai and co-workers[30], served the purpose (see figure 17). Comparatively, the difference in intensities of the AgNCs-DNA nucleobases match with the proposed mechanism being described in this paper. Even though the highest intensities were recorded with guanosine slightly higher than cytosine (figure 17).

The results of Ai and co-workers [30] and those of Yung and his group of researchers [31] are in congruent with the present study and showed weak fluorescent intensities between Ag and thymidine monophosphate.

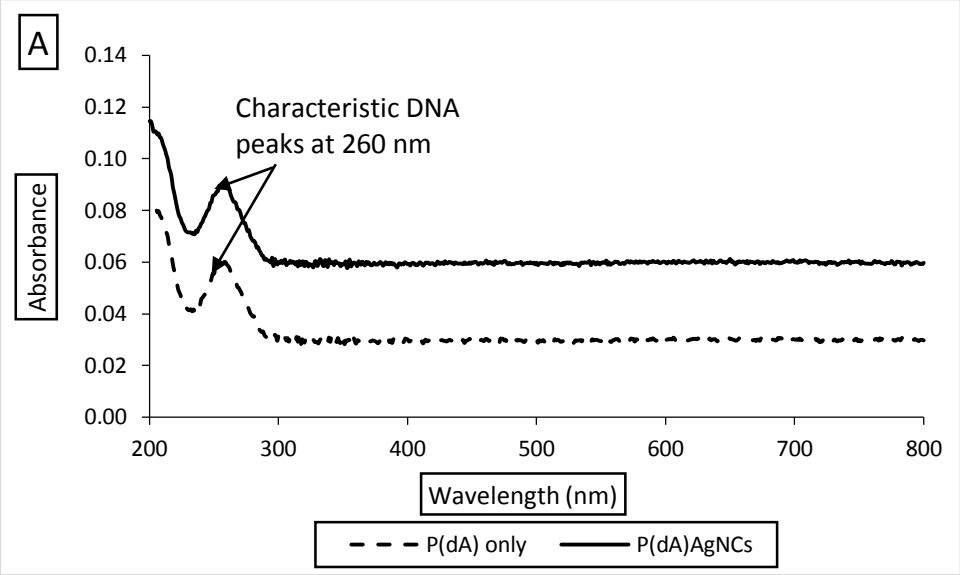

Figure 15 (a) Absorbance chart of P(dA) only (without AgBH4) and P(dA)AgNCs (with AgBH4).

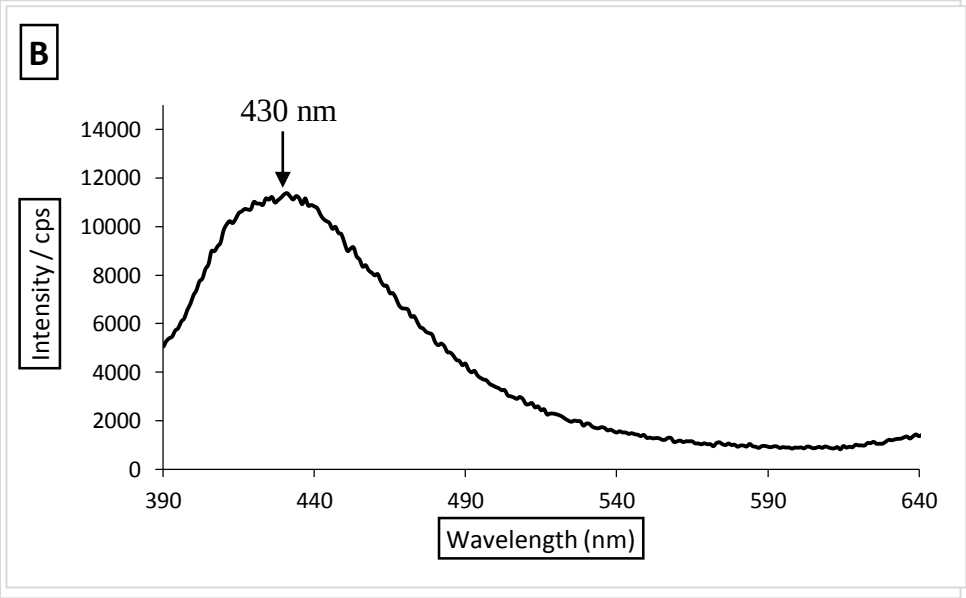

Figure 15 (b) Emission spectrum of the most intense peak (at 430nm, from an excitation of 340nm) in the spectra (a) above.

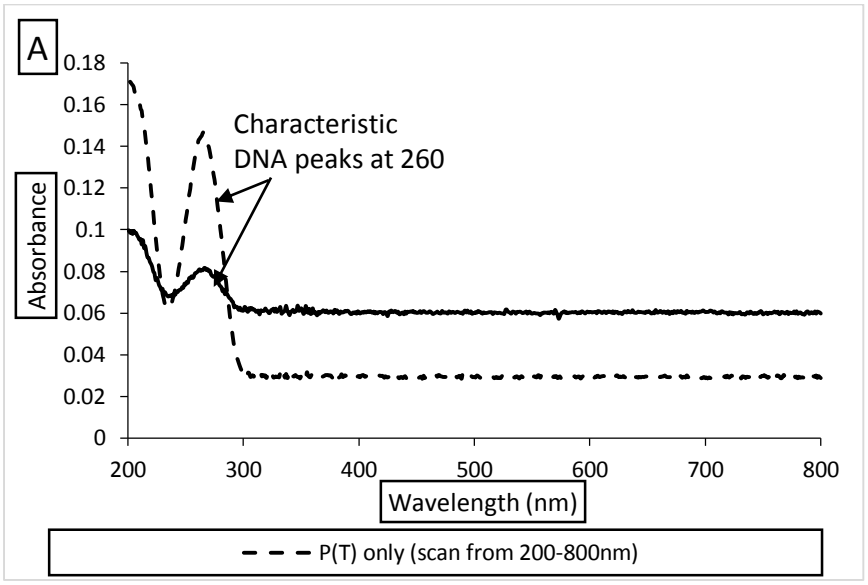

Figure 16 (a) Absorbance spectrum of P(T)AgNCs and P(T) (without AgBH4)

//

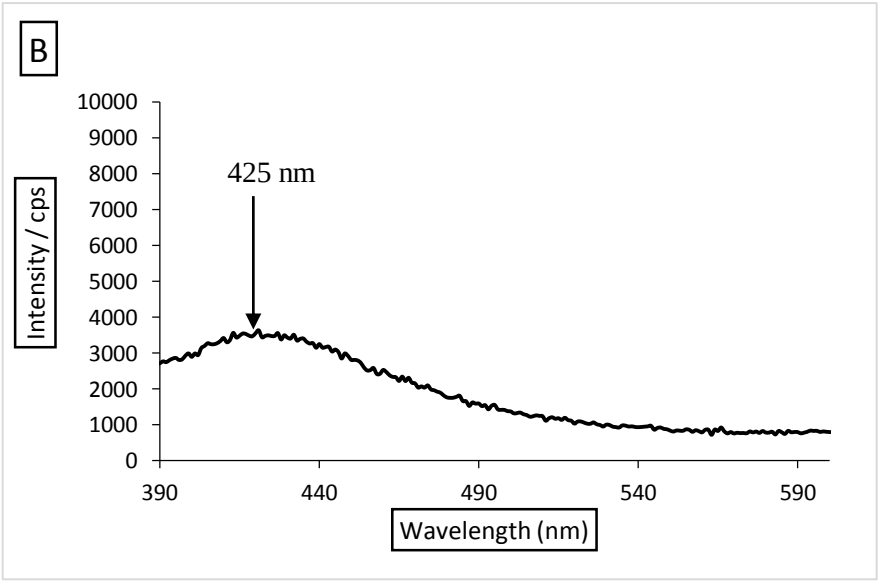

Figure 16 (b) Emission spectrum of AgNCs template on polythymine homopolymer showing weak fluorescence.

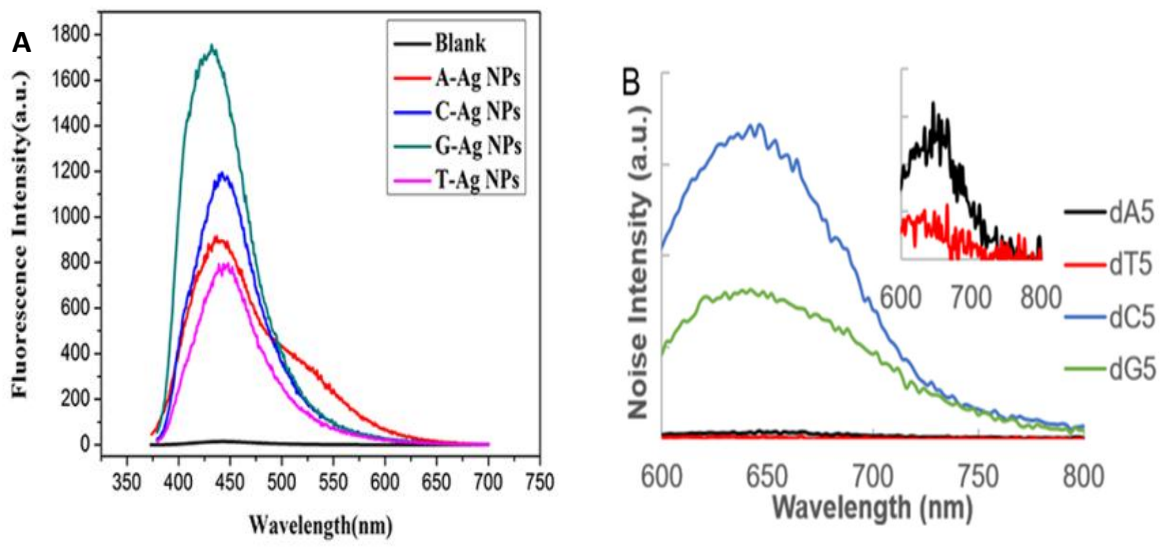

Figure 17. A) Emission spectra of Ag NCs templated on DNA nucleobases (Source: Ai *et al*.[30]). B) Fluorescence obtained for a five-nucleotide spacer length, the dark state AgNCs in absence of the activating strand was ranked as follows: C > G > A > T. Inset: Magnified background fluorescence of fully-A (black) and fully-T (red) (Source: Yung *et al*.[31]).

CONCLUSION

The binding of Ag(I) ions on DNA backbone was studied in aqueous and D_2O solutions with the view to understanding the mechanistic pathway of these reactions; using some instrumental methods to buttress the hypothesis of the reaction mechanisms. From the results obtained, it is believed that Ag(I) ions bonded with thymine nucleobase at the **T**N3 position through the lone pair electrons of the **T**N3 in a coordinate bond. The resulting bond is thought to be weak as is evident in the low fluorescence intensity of the emission spectra in figures 16 and 17. This is believed to be associated with the saturated nature of the nitrogen atom of thymine at the **T**N3 position. None of the ^{31}P NMR spectra showed any remarkable signal shifts, intensity changes, broadening or flattening out of NMR signals which illustrated that neither the carbonyl oxygen atom nor the phosphate groups were the likely binding sites for Ag(I) ions on the nucleobases. Finally, the attachment of the Ag(I) electrophile to the adenine, cytosine, and guanine nucleobases caused a significant deshielding of the **A**H8, **C**H6, **G**H8 and the **C**H1' (ribose sugar) proton signals providing further evidence of the possibility of bonding between Ag(I) ion and DNA nucleobases. All of which support the proposition that Ag(I) ions bonded to DNA bases at the **A**N3 **A**N7, **C**N3, **G**N7 positions with the electrophilic attack centred on the lone pair electrons on these nitrogen atoms. Delocalization of electrons and transfer of charges were more pronounced with the pyrimidine-ring nucleobases, particularly with cytosine. This maybe

account for the reason why cytosine is renowned for producing the most impressive luminescence effect with AgNCs of all the nucleobases in several optical studies where mono-cytosine block oligomers, cytosine-rich mixed oligomers and other DNA variants were the substrate.

REFERENCES

[1] Khan, I., Saeed, K. & Khan, I. (2019). Nanoparticles: Properties, applications and toxicities, *Arabian Journal of Chemistry*, 908-931. https://doi.org/https://doi.org/10.1016/j.arabjc.2017.05.011.

[2] Wyatt, P.J. (2018). Measuring nanoparticles in the size range to 2000 nm, *Journal, Nanoparticle Research*, 20(322), 2–18. https://doi.org/https://doi.org/10.1007/s11051-018-4397-x.

[3] Mulfinger, L., Solomon, S.D., Bahadory, M., Jeyarajasingam, A.V., Rutkowsky, S.A. & Boritz, C. (2007). Synthesis and Study of Silver Nanoparticles, Journal of Chemical Education, 84(2), 322–325. https://doi.org/10.1021/ed084p322.

[4] Hussain, A.E., Singh, I., & Singh, N.B. (2016). Green synthesis of nanoparticles and its potential application, *Biotechnology Letters*, 38(4), 545–560. https://doi.org/10.1007/s10529-015-2026-7.

[5] Alagarasi, A. (2016). *Introduction to nanomaterials*, Indian Institute of Technology, Madras, India.

[6] Gwinn, E.G., O'Neill, P., Guerrero, A.J., Bouwmeester, D. & Fygenson, D.K., (2008). Sequence-dependent fluorescence of DNA-hosted silver nanoclusters, *Advances in . Material Science*, 20(2), 279–283. https://doi.org/10.1002/adma.200702380.

[7] Cerretani, C., Kondo, J., & Swasey, S. (2020). Unusually large Stokes shift for a near-infrared emitting DNA-stabilized silver nanocluster, *Crystalline Engineering Communications*. 22(46), 8136–8141.

[8] Gonz`alez-Rosell, A., Cerretani, C., Mastracco, P., Vosch, T. & Copp, S,M. (2021). Structure and luminescence of DNA-templated silver clusters., Nanoscale Advances, 3(5), 1230–1260.

[9] Bryce, C.F.A. & Pacini, D. (1998). *The structure and function of nucleic acids.* Holbrooks Printers Ltd, Portmouth, UK.

[10] Davenport, S.G. (2006). *Anatomy and Physiology Text and Laboratory Workbook*. Link Publishing, London, UK.

[11] Huret, J.-L. (2006). DNA : molecular structure, *Genetics and Cytogenetics in*

Oncology and Haematology Atlas. 11(1), 112–123. http://atlasgeneticsoncology.org/Educ/DNAEngID30001ES.html.

[12] Kearns. D.R. & James, T. L. (1984). NMR Studies of Conformational States and Dynamics of DNA, *Critical Reviews in Biochemistry* 15(3), 237–290.

[13] Sharma, J., Rocha, R.C., Phipps, M.L., Yeh, H.-C., Balatsky, K.A., Vu, D.M., Shreve, A.P., Werner, J.H., & Martinez, J.S. (2012). A DNA-templated fluorescent silver nanocluster with enhanced stability, *Nanoscale*. 4(14), 4107–4110. https://doi.org/10.1039/c2nr30662j.

[14] Swasey, S.M., Leal, L.E., Lopez-Acevedo, O., Pavlovich, J., & Gwinn, E.G. (2015). Silver (I) as DNA glue: Ag(+)-mediated guanine pairing revealed by removing Watson-Crick constraints., *Scientific reports*. 5(4), 10163. https://doi.org/10.1038/srep10163.

[15] Santamaría-Díaz, N., Méndez-Arriaga, J.M., Salas, J.M., & Galindo, M.A. (2016). Highly Stable Double-Stranded DNA Containing Sequential Silver(I)-Mediated 7-Deazaadenine/Thymine Watson-Crick Base Pairs, *Angewante. Chemie - International Edition*, 55(21), 6170–6174. https://doi.org/10.1002/anie.201600924.

[16] Swigon, D. (2009). *Mathematics of DNA Structure, Function and Interactions*, In Benham, C.J ed.,. The IMA Volumes in Mathematics and its Applications 150 Pittsburg, USA. https://doi.org/10.1007/978-1-4419-0670-0.

[17] O'Neill, P.R., Velazquez, L.R., Dunn, D.G., Gwinn, E.G., & Fygenson, D.K. (2009). Hairpins with poly-C loops stabilize four types of fluorescent Ag n: DNA, *Journal of Physical Chemistry C*, 113(11), 4229–4233. https://doi.org/10.1021/jp809274m.

[18] Lavaee, P., Eshtiagh-Hosseini, H., HousaindokhtJoel, M.R., Mague, J. T., Esmaeili, A.A., & Abnous, K. (2016). Synthesis, Characterization and Fluorescence Properties of Zn(II) and Cu(II) Complexes: DNA Binding Study of Zn(II) Complex, *Journal of Fluorescence* 261(1), 333–344. https://doi.org/10.1007/s10895-015-1719-6.

[19] Copp, S.M., Bogdanov, P., Debord, M., Singh, A., & Gwinn, E. (2014). Base motif recognition and design of DNA templates for fluorescent silver clusters by machine learning, *Advanced Materials*. 26(33), 5839–5845. https://doi.org/10.1002/adma.201401402.

[20] Hensel, J.K., Carpenter, A.P., Ciszewski, R.K., Schabes, B.K., Kittredge, C.T., Moore, F.G. & Richmond, G.L. (2017). Molecular characterization of water and surfactant AOT at nanoemulsion surfaces, *Proceedings of the National Academy of Sciences of the United States of America*, 114(51), 13351-13356.

https://doi.org/10.1073/pnas.1700099114.

[21] Mello, L.D., Pereira, R.M.S., Sawaya, A.C.H.F., Eberlin, M.N. & Kubota, L.T. (2007). Electrochemical and spectroscopic characterization of the interaction between DNA and Cu(II)-naringin complex, *Journal of Pharmaceutical and Biomedical Analysis* 45(5), 706–713. https://doi.org/10.1016/j.jpba.2007.08.007.

[22] Copp, S.M., Schultz, D., Swasey, S., Pavlovich, J., Debord, M., Chiu, A., Olsson, K. & Gwinn, E. (2014). Magic numbers in DNA-stabilized fluorescent silver clusters lead to magic colors, *Journal of Physical Chemistry Letters*, 5(6), 959–963. https://doi.org/10.1021/jz500146q.

[23] Oyem, H.H. (2018). *Fluorescence silver nanoclusters*, Ph.D Thesis. University of Newcastle, upon Tyne, United Kingdom.

[24] Atkins, P., & de Paula, J. (2014). *Physical Chemistry*, 10th ed., Oxford University Press, London, UK.

[25] Bucak, S. & Rende, D. (2014). *Colloid and Surface Chemistry: A laboratory guide for exploration of the nano world*, 1st ed., CRC Press, Taylor & Francis Group, Boca Raton.

[26] Lakowicz, J.R. (2006). *Instrumentation for Fluorescence Spectroscopy*, Springer, New York, 1-954.

[27] Mulvaney, P., Linnert, T., & Henglein, A. (1991). Surface chemistry of colloidal silver in aqueous solution: observations on chemisorption and reactivity, *Journal of Physical Chemistry*, 95(20), 7843–7846. https://doi.org/10.1021/j100173a053.

[28] Fischer, S. A., Crotty, A.M., Kilina, S. V., Ivanov, S. A. & Tretiak, S. (2012). Passivating ligand and solvent contributions to the electronic properties of semiconductor nanocrystals, *Nanoscale*. 4(3), 1-904. https://doi.org/10.1039/c2nr11398h.

[29] Petty, J.T., Zheng, J., Hud, N. V. & Dickson, R.M. (2004). DNA-Templated Ag Nanocluster Formation, *Journal of the American Chemical Society*, 126(16), 5207–5212. https://doi.org/10.1021/ja031931o.

[30] Nie, F., Ga, L., & Ai, J. (2019). One-Pot Synthesis of Nucleoside-Templated Fluorescent Silver Nanoparticles and Gold Nanoparticles, *ACS Omega*, 4(4), 7643–7649. https://doi.org/10.1021/acsomega.9b00701.

[31] Ang, Y.S., Wen, W., Woon, E. & Yung, L.L. (2018). The role of spacer sequence in modulating turn-on fluorescence of DNA-templated silver nanoclusters, *Nucleic Acids Research*, 46(14), 6974–6982. https://doi.org/10.1093/nar/gky521.